Experimental Investigation and Finite Element Simulation of laser lap welding of SS304 sheets

N. Siva Shanmugam, G. Buvanashekaran and K. Sankaranarayanasamy

***Abstract*—**Laser beam welding (LBW) is one of the most important manufacturing processes used for joining of materials. It is also a remarkably complicated, nonlinear operation involving extremely high temperatures. Since its invention more than two decades ago, laser beam welding has been more of an art than a science. Laser welding of austenitic stainless steel AISI 304 the candidate material of this research work is used in several areas, including electronics, medical instruments, home appliances, automotive and specialized tube industry. An industrial 2kW CW Nd:YAG laser system, available at Welding Research Institute (WRI), BHEL Tiruchirappalli, is used for conducting the welding trials for this research. After proper tuning of laser beam, laser welding experiments are conducted on AISI 304 grade sheets for lap joint configuration to evaluate the influence of input parameters such as beam power, welding speed and spot diameter of the beam on weld bead geometry i.e. bead width (BW) and depth of penetration (DOP). Three dimensional finite element simulation of high density heat source is performed for laser welding technique using finite element code SYSWELD for predicting the temperature profile on AISI 304 stainless steel sheets. The temperature dependent material properties for AISI 304 stainless steel are taken into account in the simulation, which has a great influence in computing the temperature profiles. The latent heat of fusion is considered by the thermal enthalpy of material for calculation of phase transition problem. A Gaussian distribution of heat flux using a moving heat source with a conical shape is used for analyzing the temperature profiles. Experimental and simulated values for weld bead profiles are analyzed for stainless steel material for different beam power, welding speed and beam spot diameter. The results obtained from the simulation are compared with those from the experimental data for laser welding of lap joint configuration and it is observed that the results of numerical analysis (FEM) are in good agreement with experimental results, with an overall percentage of error estimated to be within ±5%.

***Keywords*—**Nd:YAG Laser welding, Heat source, SS 304, lap joint.

I. Introduction

LASER Beam Welding (LBW) is a modern welding process (high energy density process) that continues to expand into modern industries and new applications because of its major advantages like deep weld penetration and minimizing heat inputs [1]. In general, laser welding generally is a keyhole fusion welding technique which is achieved with the very high power density obtained by focusing a beam of laser light to a very fine spot. At a focused power density in the order of 10^5 W/cm^2, the rapid removal of metal by vaporization initiates a small keyhole into a workpiece. As the keyhole propagates deeper into the workpiece, the laser light is scattered repeatedly within it, thus increasing the coupling of laser energy into the work.

At a relatively low power density of laser beam of about 10^3 W/cm^2, the energy is absorbed at the surface and is conducted into the interior of the work piece by thermal conduction. This is relatively a slow process and at this level, the welds tend to be shallow and wide. Hence, the weld penetration depth is less compared to the weld bead width. This regime is often called conduction limited welding. In contrast, at power densities in the order of $10^5 – 10^6$ W/cm^2, the welds are deep and narrow, resulting in keyhole welding requiring short interaction times, thus promoting high welding speeds. Hence, laser welding is a complex welding process which often requires several preliminary studies and experimental trials prior to accomplishment of accurate results. Typically, welding were carried out by the skilled workers, nowadays with the advent of modern scientific technology, automated machines and robots are introduced in welding process for various industrial sectors like automobile, ship-building, aerospace, defence/military, research etc. These are the industrial sectors where the expected productivity must be achieved and the parts to be assembled require high precision. To achieve the expected productivity and high-quality products, the accuracy control in welding should be maintained. The concept of accuracy control in welding should be maintained in the structural design phase, so that the designer can produce a better designed product.

Computer based Finite Element (FE) simulation of welding process is widely employed in research, predominantly in the design phase [2-5]. But there is a wide gap between the computer based FE simulation and welding process notably in autogenous welding process like laser. Meanwhile, there is a large need in for more theoretical prediction of weld bead geometries for lap seam joint configuration exclusively in the automobile applications. This research work focuses on the finite element simulation and experimental analysis of laser welding process of AISI 304 stainless steel sheet, the most viable material in automobile applications and the boiler components.

The literature that focuses mainly on terminologies/methodologies dealing with austenitic stainless

N. Siva Shanmugam is with the Department of Mechanical Engineering, National Institute of Technology, Tiruchirappalli 620015, Tamil Nadu, INDIA (corresponding author phone: +91-431-2503425; fax: +91-431-2500133; e-mail: nsiva@nitt.edu).

G. Buvanashekaran is with the Welding Research Institute, Bharat Heavy Electricals Limited, Tiruchirappalli 620014, Tamil Nadu, INDIA (e-mail: gbs@bheltry.co.in).

K. Sankaranarayanasamy is with the Department of Mechanical Engineering, National Institute of Technology, Tiruchirappalli 620015, Tamil Nadu, INDIA (e-mail: ksnsamy@nitt.edu).

steel sheet welding and its corresponding FE models are briefly presented here. Monem and Batahgy [6] evaluated the fusion zone shape and final solidification structure of different types of austenitic stainless steels (304L, 316L and 347) with different thicknesses (3 and 5 mm) as a function of laser parameters. Laser welding of thin sheets of AISI 304 stainless steel was carried out by Nath et al [7] with high power CW CO_2 laser. In order to estimate the coupling efficiency and determine various laser welding process parameters for good quality welds, bead-on-plate welding of AISI 304 stainless steel sheets of various thickness in 0.1–1.55 mm range in both conduction and keyhole welding modes were carried out. Fuerschbach and Eisler [8] studied experimentally, the effects of process parameters such as pulse energy, duration and spot size on melting, weld appearance and heat input for the pulsed Nd:YAG laser spot welding of AISI 304 stainless steel. The research activity in the laser welding simulation started a decade ago. The elementary welding heat source models were based mostly on Rosenthal's solutions [9]. The residual stresses and strains in a rectangular thick AISI 304 stainless steel plate during CO_2 laser welding process were investigated by Carmignani et al. [10] using finite element code ABAQUS. The bead shape in pulsed Nd:YAG laser spot welding of thin 304 stainless steel sheets was predicted by Chang and Na [11] using finite element method and neural network. Sabbaghzadeh et al. [12] developed two numerical models based on finite difference method and finite element method to compute the thermal phenomena during welding of AISI 304 stainless steel sheet using pulsed Nd:YAG laser. There are many research papers [6-13] which deal with the shape and size of the molten pool of laser beam butt welds in relation to different laser input parameters. However, the effect of main laser parameters namely beam power, welding speed and beam spot diameter on lap joint welds have till date not been reported in detail. Since the sheets are placed one and another in lap joint configuration, the beam should penetrate the top sheet and get into the bottom sheet. Hence, the effect of beam spot diameter on weld bead geometry has to be analyzed in depth.

This paper presents the thermal field and the bead shape of a lap joint made of AISI304 stainless steel sheet by laser welding, using FE transient thermal analysis. The heat source model is assumed to be a 3D conical Gaussian and the required FORTRAN subroutines are developed in order to define a moving distributed heat source for the simulations carried out using finite element code SYSWELD. The depth of penetration and bead width of lap joint laser welds obtained by simulation methods are compared with the lap joints weld specimens produced using the same welding parameters for validation.

II. Heat Transfer Analysis

To identify the relationships between the molten pool shape and the laser welding parameters, it is necessary to first study the effects of the laser process parameters on the temperature field induced by laser irradiation. The coordinate system of laser welding used in this work is shown in Fig. 1. It is assumed that a laser beam with Conical Gaussian distribution [14] moves with a constant velocity v along the x-axis. In general, the governing equation of heat conduction for the three dimensional transient temperature can be written as :

$$\rho(T)c(T)\frac{\delta T}{\delta t}+v\rho(T)c(T)\frac{\delta T}{\delta x}=\frac{\delta}{\delta x}\left(k_x\frac{\delta T}{\delta x}\right)+\frac{\delta}{\delta y}\left(k_y\frac{\delta T}{\delta y}\right)+\frac{\delta}{\delta z}\left(k_z\frac{\delta T}{\delta z}\right)+\text{heat source} \quad (1)$$

where T is the temperature (^oC), which is a function of x, y, z and time t in seconds (s), ρ is the density of the material (kg/mm^3), k_x, k_y and k_z are the thermal conductivity in the x, y and z directions, respectively, (W/mm ^oC) and c is the specific heat capacity (J/kg ^oC). The above said physical properties are temperature dependent. The heat source is expressed as heat generation per unit volume (J/mm^3).

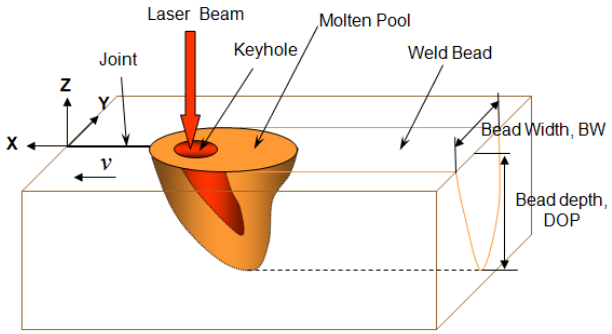

Fig.1 Schematic representation of coordinate system of laser welding process

A. Boundary Conditions

In order to solve the above differential equation, boundary and initial conditions must be specified. A boundary condition may be either absolute (prescribed temperature) or natural (prescribed thermal fluxes) and also being a function of time.

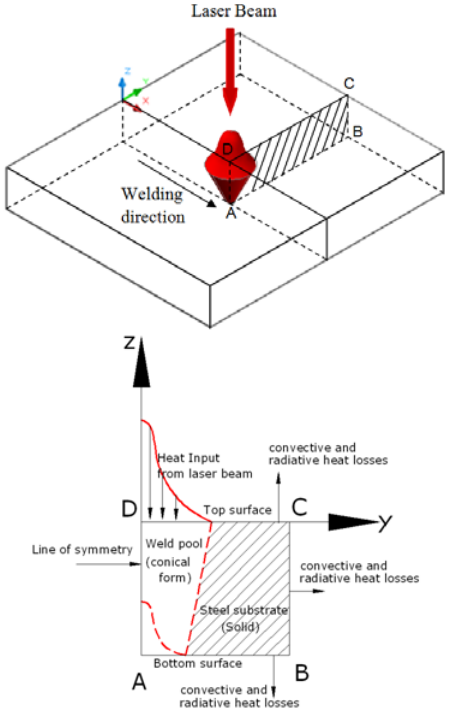

Fig. 2 Schematic representation of thermal boundary conditions

Fig. 2 illustrates the thermal boundary conditions on a typical transverse section A-B-C-D. The focused laser beam is irradiated on the top surface within a circular zone defined by the position of centre of the laser beam and its effective radius. The rest of the steel substrate surface facing air is subjected to the convection and radiative heat losses. If T_0 is the atmospheric temperature or room temperature, the initial condition is:

$$T(0,y,z,t) = T_0(x,y,z) \quad (2)$$

The essential boundary condition for the transient analysis is

$$T(x,y,z,0) = T_0(x,y,z) \quad (3)$$

The boundary conditions for the heat transfer coefficient h are divided into radiation and convection. Given a body temperature T, radiation to the surrounding medium Q''_{rad} at the temperature T_0 follows the Stefan-Boltzmann law. The resulting temperature difference causes a flux (power loss) which can be expressed as:

$$Q''_{rad} = \sigma\varepsilon(T^4 - T_0^4) \quad (4)$$

$$= \sigma\varepsilon(T^2 + T_0^2)(T + T_0)(T - T_0) \quad (5)$$

$$= h_{rad}(T - T_0) \quad (6)$$

where ε is the surface emissivity, σ is the Stefan-Boltzmann constant and h_{rad} is the resulting temperature dependent heat transfer coefficient for radiation. Given a body with temperature T, surrounded by a fluid or gas at temperature T_0, heat convection assumes that a thermal layer exists with the heat transfer coefficient h_{con}, so the resulting temperature difference across the boundary layer causes a flux, Q''_{con}, and is written as

$$Q''_{con} = h_{con}(T - T_0) \quad (7)$$

B. Heat Source Modeling

In laser welding process, a part of the energy generated by the laser source is lost before absorbed by the weld specimen. The energy loss is due to the reflection from the specimen surface while rest of the energy is absorbed by the specimen. The energy loss for AISI304 stainless steel material determined experimentally by the past researchers [15] is 30.7% of the nominal power of the laser source [10]. Therefore, the absorbed energy considered for this present investigation is 69.3% of the beam power.

During simulation, consideration is given to the fact that the heat comprises a plane heat source on the top surface and a conical heat source along the thickness direction (refer Fig. 3). In that 69.3% of the beam power, the power absorbed on the surface of the specimen is 17.3% (Q_{surf}) and the remaining 52.7% by the keyhole wall ($Q_{keyhole}$). Assuming that the laser beam maintains a constant Transverse Electromagnetic mode (TEM_{00}), the Gaussian heat flux distribution $Q(x,y)$ can be expressed as:

$$Q(x,y) = \frac{3Q_{surf}}{\pi R^2} exp\left(-\frac{3(x^2+y^2)}{R^2}\right) \quad (8)$$

where Q_{surf} is heat power of the plane heat source (17.3%) and R is the heat source radius.

The radius of the heat source is calculated from the focal length of the focusing lens, which can be computed according to the relation found in

$$R = \frac{2M_0^2\lambda F}{\pi D_0} \quad (9)$$

where M_0^2 is the value of beam quality (Nd:YAG laser with a wavelength (λ) of 1.060 µm, beam quality is 1.04), F is the focal length of the focusing lens and D_0 is the minimum diameter of the laser beam (0.3 mm). Assuming the simulation of keyhole is a cone, the Gaussian distribution of heat flux is written as

$$Q(z) = \frac{2Q_{keyhole}}{\pi r_0^2 H} e^{1-\left(r/r_0\right)^2}\left(1 - \frac{z}{H}\right) \quad (10)$$

where $Q_{keyhole}$ is the absorbed laser beam power (52%), r_0 is the initial radius (at the top of the keyhole - 0.3 mm), H is the sheet thickness, r is the current radius, i.e. the distance from the cone axis and z is the current depth [16]. The total heat input to the model is computed from the summation of surface and volume heat source models.

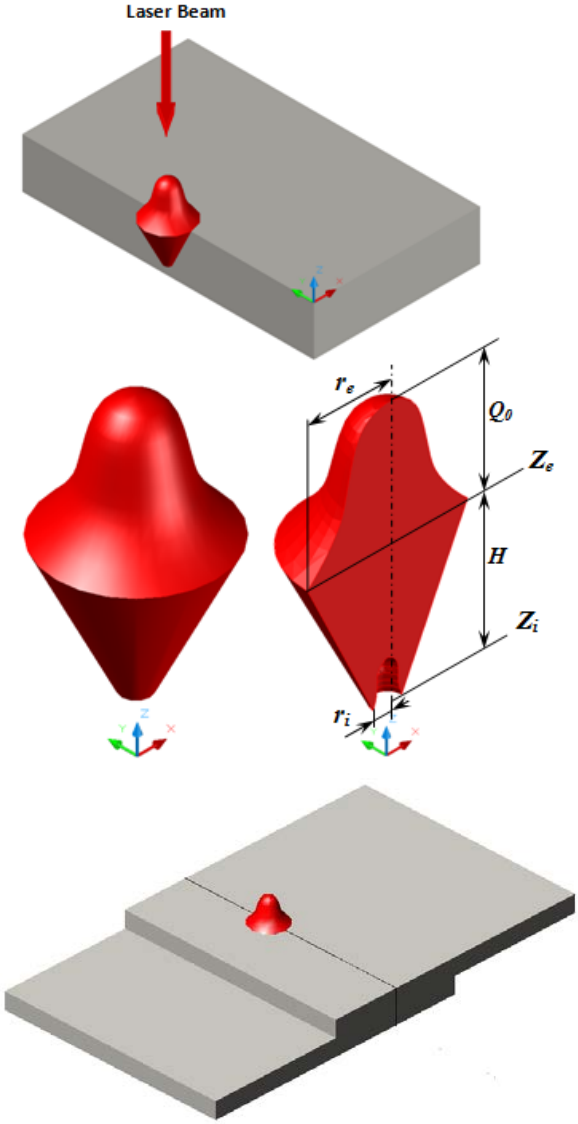

Fig. 3 Schematic of 3D Conical Heat source model

C. Heat Source Fitting

In this research work, a three dimensional conical Gaussian heat source (volumetric heat source) is adapted as a laser source and it is applied to specific elements in the finite

element model. The heat source representation is defined using the SYSWELD heat source fitting tool as shown in Figs. 4 for lap joint configuration. The laser heat source is fitted in such a way that the start position of the weld is defined with respect to the weld trajectory or line.

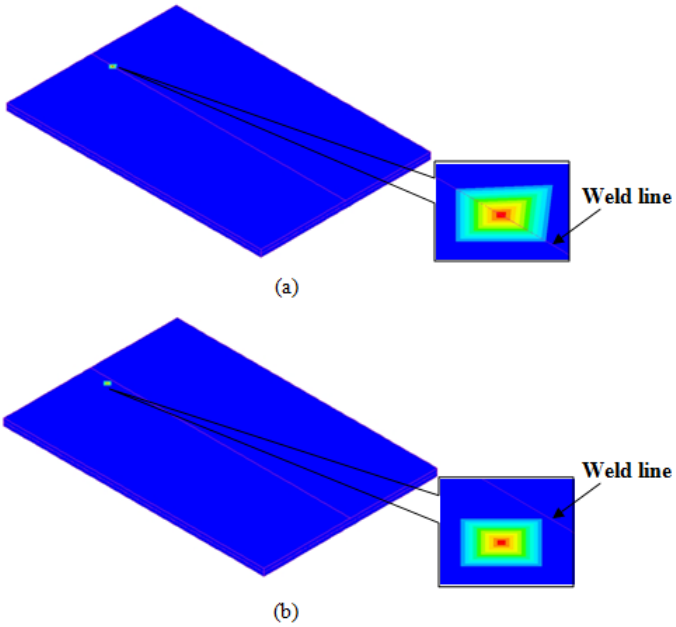

Fig. 4 Heat source fitting (a) in the weld line and (b) offset from the weld line

The finite element code, SYSWELD has the capability of defining the heat source with respect to a moving reference point in the weld line. It is also possible in SYSWELD to define the (refer Figs. 4 (a)-(b)) offset of the heat source centre (x_0,y_0,z_0) and the angle of the laser beam relative to z axis and oriented by either y axis (a_y) or x axis (a_x). The source intensity Q_v is calculated based on distance from a moving reference point to all nodes in the local area, according to Eqs. 8 and 10 presented in section B. This moving load is implemented through a FORTRAN subroutine [16].

III. Finite Element Analysis

Several complex thermal and metallurgical phenomena occurring simultaneously during welding can be captured through a proper FE model. This section presents the 3D FE simulation for the lap joint configuration to determine the temperature distribution and weld bead geometry in each, using SYSWELD FE software.

A. Finite Element Modeling

Three dimensional finite element model is developed for lap joint configuration to simulate the laser welding process using the commercial code SYSWELD. The models are used to predict the temperature distribution and weld geometry for the laser welding process of a thin walled structure (sheet) of AISI 304 stainless steel (SS304). The geometry and finite element mesh used in the model are given in Table 1.

Table 1: Finite element mesh and geometry to simulate the laser welding process for lap joint configuration

No. of Nodes – 55927
No. of Elements – 50362

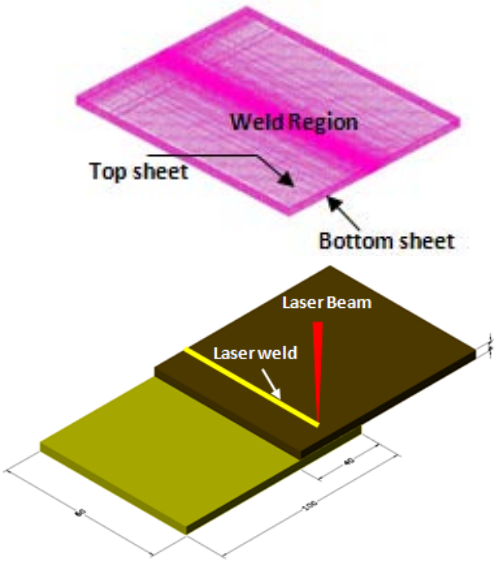

The whole solution domain is discretized into uniform 8-node hexahedron elements. The accuracy of the finite element solution depends upon the density of the mesh used in the analysis. The temperature around the laser beam is higher than the boiling point of the material and it drops sharply in regions away from the molten pool or fusion zone. Therefore, in order to obtain the correct temperature field in the laser irradiation region it is necessary to have a dense mesh close to the weld area while in regions located away from weld area a coarse mesh is used. This will help in obtaining a reasonably accurate solution within a short time. In the analysis, the phase transformation is considered since the peak temperature reaches the boiling point of the steel substrate. The convection and radiation loads are applied as surface loads on the element-free faces, specifying the film coefficient, ambient temperature and emissivity of the material. Temperature dependent material properties of AISI 304 stainless steel are specified to conduct the non-linear transient thermal analysis. The following assumptions are made while developing the finite element model:

- The workpiece initial temperature is 30°C.
- Thermal properties of the material such as conductivity, specific heat, density are temperature dependent.
- The convection and radiation loads are considered.
- There is no predefined weld bead geometry.
- In lap joint configuration, the lapped region alone is considered for the analysis purpose.

B. Material Model

The material used for this purpose is commercial AISI304 stainless steel sheet of thicknesses 1.0 and 1.6mm. The chemical composition of this material under annealed

condition is presented in Table 2. Thermo-physical properties (temperature dependent) of the material are assumed to be isotropic and homogeneous and are taken according to Sabbaghzadeh et al [8]. The latent heat of fusion is 247 kJ/kg, to be released or absorbed over the range of temperature between T_S = 1400°C and T_L = 1500°C and the latent heat of vaporization is 7600 kJ/kg [5] (above 2467°C).

Table 2: Chemical composition of AISI304 stainless sheet metal vs. the weight percentage

C	Cr	Fe	Mn	Ni	P	S	Si
0.055	18.28	66.34	1.00	8.48	0.029	0.005	0.6

IV. Laser Welding Parameters

A GSI Lumonics JK2000 Nd:YAG laser welding system available at WRI, BHEL, Trichy is employed for the present study (refer Fig. 5). The welding parameters chosen for the analysis are listed in the Table 3. The parameters are selected based on the expertise available at Welding Research Institute, BHEL, Trichy, where laser welding was successfully used for many industrial applications like welding of fins, batteries, dental clips etc.

Fig. 5 Nd:YAG laser welding torch

Table 3: Laser welding parameters

Sl. No.	Beam Power (BP), watts	Welding Speed (WS), mm/min	Beam Angle (BA), deg.	Focal Length (F), mm
1	1000	500	85	120
2		600		
3	1250	700		
4		800		160
5	1500	900		
6		1000		

V. Results And Discussions

FE simulations using SYSWELD for lap joints are run for the combinations of laser welding parameters adopted for experimental trials. Hence, the validation of computed results from FE model and general applicability of adaptive volumetric heat source is ensured. In addition, the finite element model is also validated with a set of experimentally measured lap joint weld dimensions.

Finite element simulation of lap joint welding is carried out for each welding condition listed in Table 3 to determine the weld geometry, i.e. bead width and depth of penetration taking the material properties for 1.0 mm thick AISI 304 SS sheets. Fig. 6 presents the temperature contours at four different time periods during the laser irradiation for one of the cases, where the beam power is 1250 W, welding speed is 700 mm/min and the beam angle is 85°, from which the high temperature gradients in the vicinity of the weld line close to the laser source may be clearly observed.

The heat inputs generated by the moving heat source along the weld line are gradually transferred in all directions of the sheet by conduction, convection and radiation. As can be seen from the figure, the temperature around the laser source reaches around 3934°C suggesting vaporization of material in the fusion zone. However, the temperature around the edge where the welding is started is decreased greatly to the range of 997°C. It can be seen that the laser source preheats a very small area in front of the laser source where the heat source is going to pass.

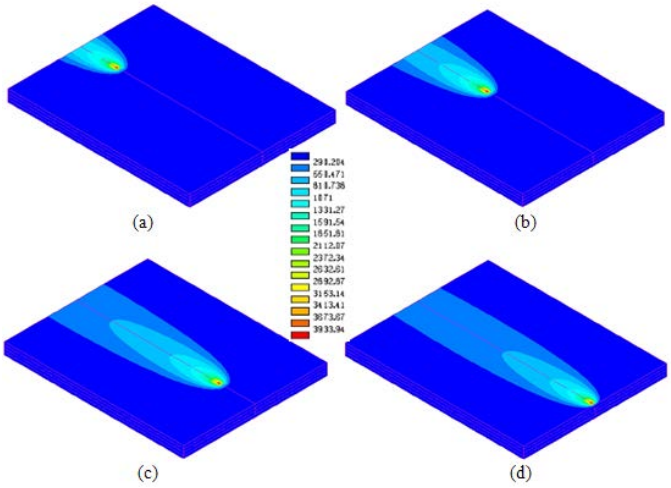

Fig. 6 Temperature distributions during the welding process at four different time periods (a) 1.28 s, (b) 2.49 s, (c) 4.50 s and (d) 5.85 s

The influence of the beam power on the bead shape with a fixed welding speed of 700 mm/min and spot diameter of 0.8 mm is shown in Fig. 7. From this result, one can infer that both the penetration depth and bead width increases as beam power increases. From the simulation result, it is observed that at higher beam power (1500 W) proper fusion of top and bottom sheets are achieved, whereas at lower beam power (1000 W) the top sheet alone is melted and there is no penetration in the bottom sheet. Further, the increase in beam power leads to an increase in the heat input, therefore, more

molten metal and consequently more penetration depth is achieved. However, the idea is reversed in the case of weld speed effect, because the welding speed has an opposite effect to that of beam power.

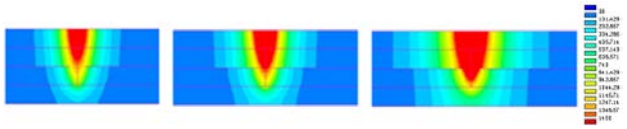

Fig. 7 Effect of beam power (a) 1000 W, (b) 1250 W and (c) 1500 W on weld bead geometry at constant welding speed of 700 mm/min and spot diameter of 0.8 mm

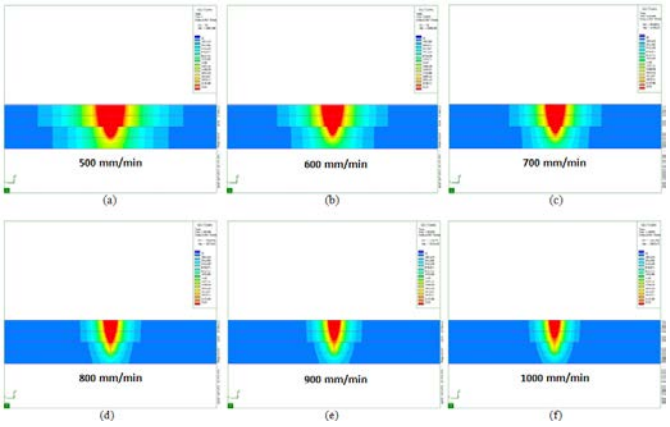

Fig. 8 Effect of welding speed on weld bead geometry at constant beam power of 1500 W and spot diameter of 0.8 mm

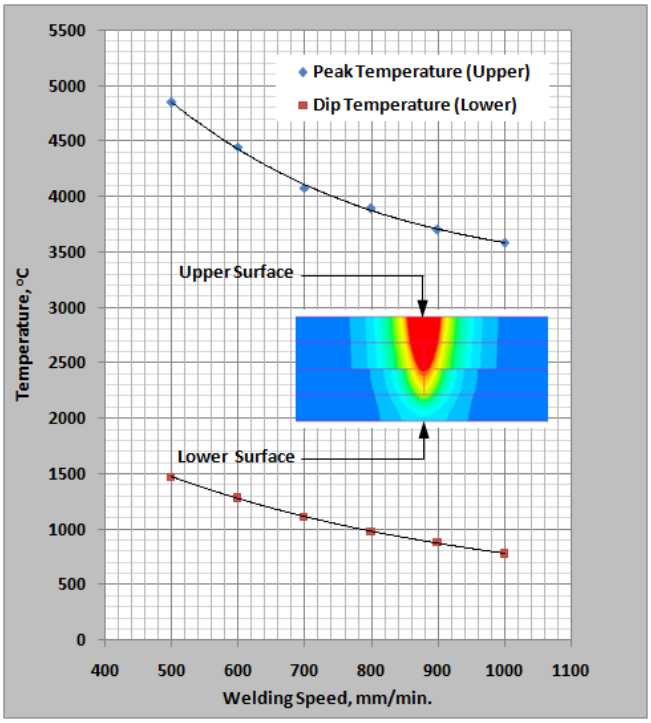

Fig. 9 Effect of welding speed on peak and dip temperature values for beam power of 1250 W and spot diameter of 0.8 mm

Fig. 8 shows the dependence of the welding penetration depth and bead width on the welding speed for a beam power of 1500 W and spot diameter of 0.8 mm. The trend of decrease in penetration depth and bead width with increase of the welding speed can be noticed. It can be explained by the fact that the amount of heat conduction transmitted to the base metal decreasing as the welding speed increases. From the point of view of physical phenomena, the reduction of the welding speed results in increased interaction time between the laser beam and component material. This time expansion caused the increase of the maximum temperature value and heat input along thickness causing a greater volume to be melted.

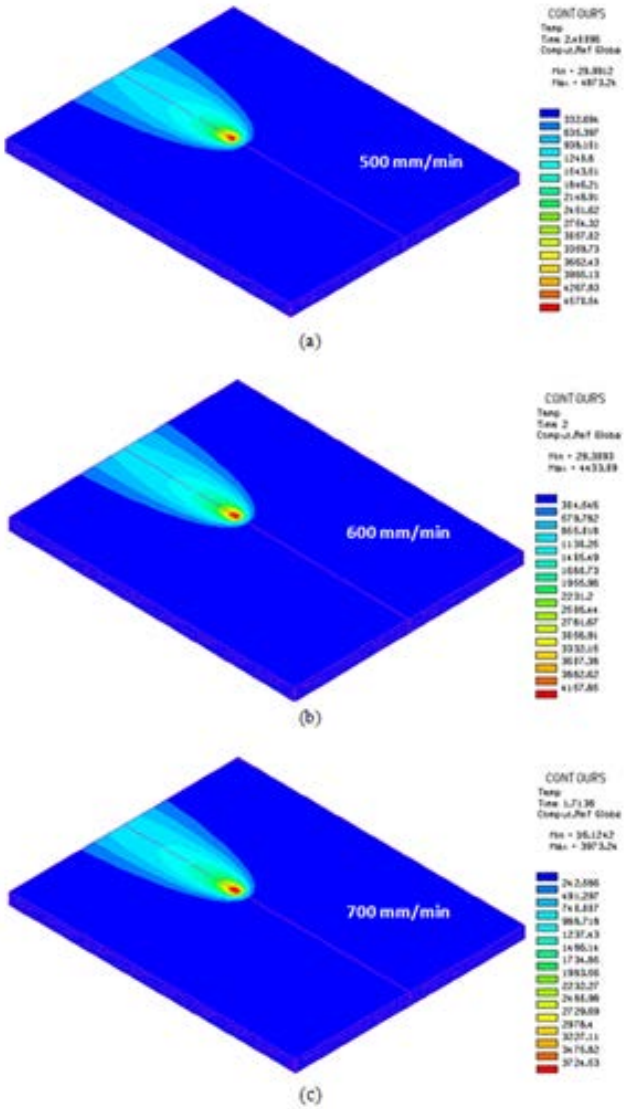

Fig. 10 (a-c) Temperature distributions at various welding speeds (beam power – 1250 W and spot diameter - 0.8 mm)

Following the same analogy, the increase of welding speed reduced the peak temperature values (refer Fig. 9) of the upper and the lower surface of the workpiece and heat conduction along thickness, with a reduction of the molten volume. Obviously, the peak values and the temperature gradient are increased with decrease in the welding speed, but the relationship between them is non-linear. The analysis is then

extended to evaluate the speed effect on the bead profiles for welding speeds varying from 500 mm/min to 700 mm/min while the other process parameters are kept constant (refer Fig. 10). From the point of view of physical phenomena, the reduction of the welding speed results in increased interaction time between the laser beam and component material. This time expansion caused the increase of the maximum temperature value and heat input along thickness causing a greater volume to be melted. As a result, the heating or welding tail is longer and wider while penetration is deeper.

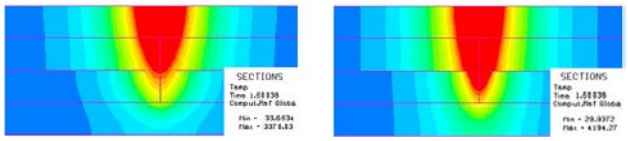

(a) (b)

Fig. 11 Effect of Spot diameter (a) 0.8 mm and (b) 0.6 mm on weld bead geometries at constant beam power of 1500 W and welding speed of 1000 mm/min

Fig. 11 shows typical result of the effect of spot diameter on weld bead geometry for specimen thicknesses of 1.0 + 1.0 mm. It is observed that a focused beam of small diameter (0.6 mm) results in increase in the power density of the beam, resulting in better penetration depth. Once the spot diameter of the beam is increased, the laser beam becomes wider resulting in the beam energy exposed to wide area. Therefore, wide area of the base metal will melt leading to an increase in bead width. To achieve maximum penetration depth the beam power has to be maintained at higher level with minimum spot diameter of the beam, while welding speed has to be minimum.

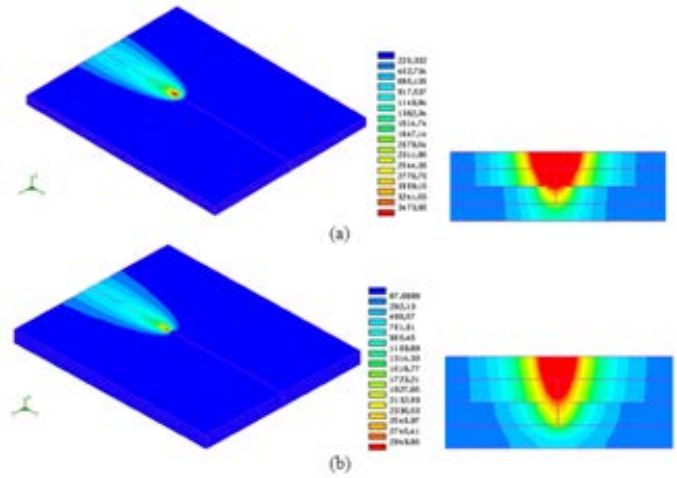

Fig. 12 Temperature distributions during the welding process at two different workpiece thicknesses (a) 1.0 mm and 1.6 mm

Figs. 12 (a) and (b) show results for the effects of workpiece thickness on temperature distribution for beam power of 1500W, welding speed of 900 mm/min and spot diameter of 0.8 mm. It is seen that temperature decreases as the thickness of the workpiece increases. It is also noted that the temperature in the x- and z-directions decreases as the workpiece thickness increases. Both the peak temperature and the temperature gradient decrease as the workpiece thickness increases. This is due to the fact that the heat transfer rate is higher in high thickness workpiece compared to low thickness workpiece.

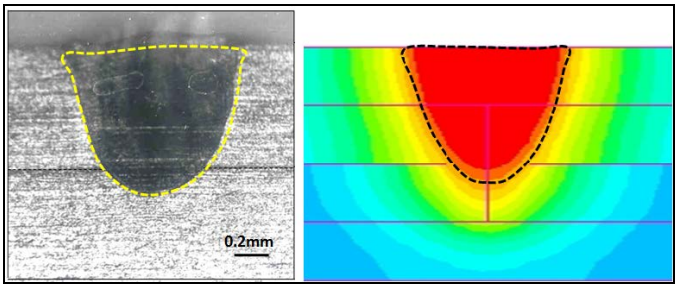

(a) (b)

Fig. 13 Comparison of calculated result with experimental one for beam power of 1250 W, welding speed of 800 mm/min and spot diameter of 0.8 mm and workpiece thickness of 1.0+1.0mm
(a) Sectioned specimen and (b) Contour of calculated melting temperature

Fig. 13 shows comparison of cross section of bead profile obtained from experiment and simulation for the thickness combination of 1.0 + 1.0 mm with beam power of 1250 W and welding speed of 800 mm/min. The comparison shows that the bead width and penetration depth calculated by simulation agree well with the experimental result with an error of about 2%.

Fig. 14 shows the comparison between the calculated and the corresponding measured weld pool dimensions i.e. bead width and penetration depth for all cases of the beam powers and welding speeds considered in the present work.

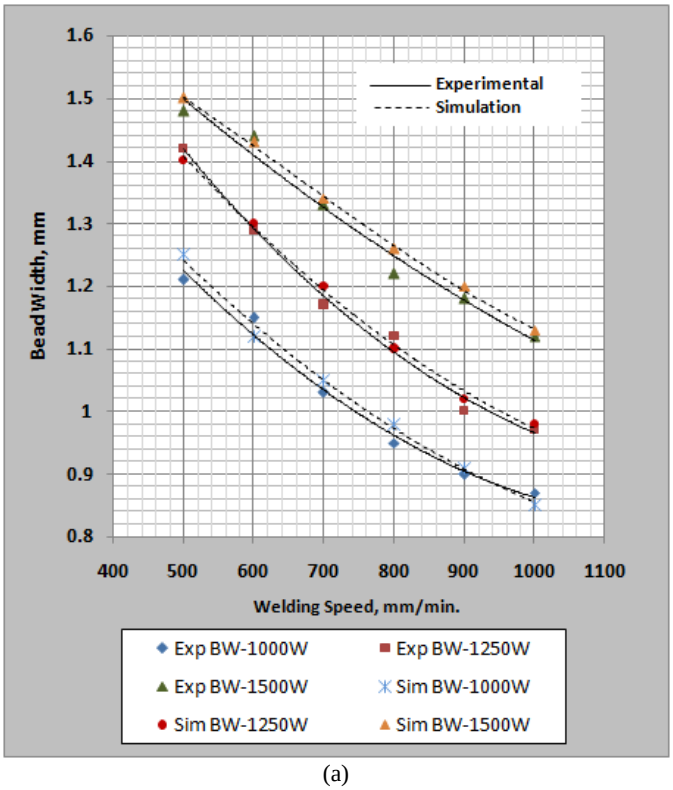

(a)

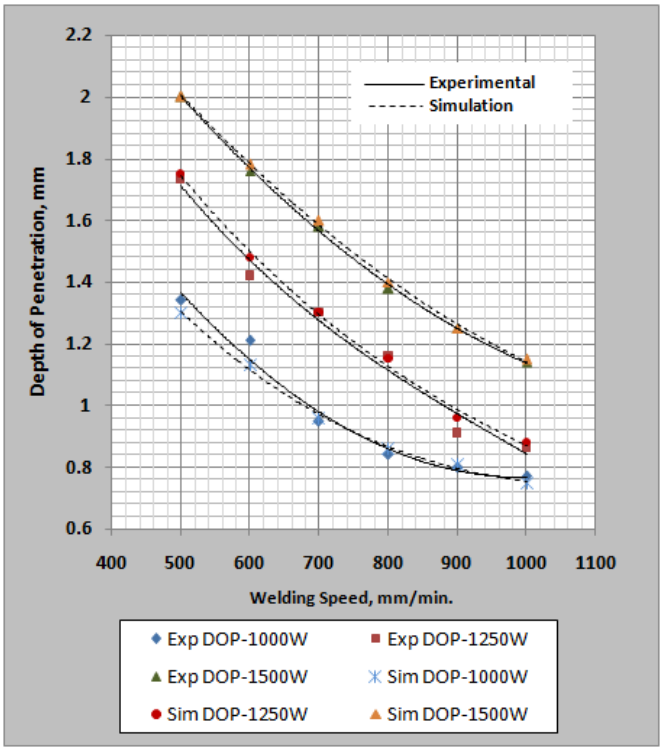

(b)

Fig. 14 Comparison of computed weld dimensions (a) Bead width and (b) Depth of penetration with corresponding measured results

It can be observed from Fig. 14 (a) and (b) that the bead width and penetration depth decrease linearly with the increase in the welding speed. The bead width decreases from 1.5 to 1.13 mm and decrease in the penetration depth from 2 to 1.15mm with increasing welding speed from 500 to 1000 mm/min at a constant beam power of 1500 W, spot diameter of 0.8 mm and specimen thickness of 1.0 + 1.0 mm. Further, it is concluded from the results that the FEM simulations predict the penetration depth and bead width within a maximum error of about ±5%. A similar type of observation is also noticed for another thickness combination of 1.6 + 1.6 mm considered in this work.

ACKNOWLEDGMENT

The authors thank Head and Management of Welding Research Institute (WRI), Bharat Heavy Electricals Limited, Tiruchirappalli, India for extending the lab facilities to carry out this research work and allowing to present the results in this paper. Authors thank NITT for providing computation facilities (SYSWELD).

REFERENCES

[1] T.L. Teng, C.P. Fung, P.H. Chang and W.C. Yang, Analysis of residual stresses and distortions in T-joint fillet welds, *International Journal of Pressure Vessels and Piping*, 78, pp. 523-538, 2001.

[2] A. Moarrefzadeh and M.A. Sadeghi, "Numerical simulation of copper temperature field in Gas Tungsten Arc Welding (GTAW) process (Published Conference Proceedings style)," in *Proceedings of the 10th WSEAS International Conference on Robotics, Control and Manufacturing Technology*, China, 2010, pp. 26-31.

[3] D. Gabriela, D. Mihai, G. Luminita and G. Valentin, "Simulation of Temperature Field on Steels during Laser Hardening (Published Conference Proceedings style)," in *Proceedings of the 2nd WSEAS International Conference on Engineering Mechanics, Structures and Engineering Geology*, Greece, 2009, pp. 229-232.

[4] I. S. Leoveanu and D. Taus, "Modelling the transport phenomenon involved in the fusion-welded (Published Conference Proceedings style)," in *Proceedings of the 4th European Computing Conference*, Romania, 2010, pp. 63-68.

[5] M. Bachmann, V. Avilov, A. Gumenyuk and M. Rethmeier, "CFD Simulation of the Liquid Metal Flow in High Power Laser Welding of Aluminum with Electromagnetic Weld Pool Support (Published Conference Proceedings style)," *Recent Researches in Mechanics*, Greece, 2011, pp. 179-184.

[6] A. Monem and E. Batahgy, Effect of laser welding parameters on fusion zone shape and solidification structure of austenitic stainless steels, *Journal of Material Letters*, 32, pp. 155-163, 1997.

[7] A.K. Nath, R. Sridhar, P. Ganesh and R. Kaul, Laser power coupling efficiency in conduction and keyhole welding of austenitic stainless steel, *Sadhana*, 27(3), pp. 383-392, 2002.

[8] P.W. Fuerschbach and G.R. Eisler, Effect of laser spot weld energy and duration on melting and absorption, *Science and Technology of Welding and Joining*, 7(4), pp. 241-246, 2002.

[9] D. Rosenthal, The Theory of Moving Source of Heat and it's Application to Metal Treatment,' *Trans. ASME*, 68, pp. 849–866, 1946.

[10] C. Carmignani, R. Mares and G. Toselli, Transient finite element analysis of deep penetration laser welding process in a singlepass butt-welded thick steel plate, *Journal of Computational Methods in Applied Mechanics and Engineering*, 179, pp. 197-124, 1999.

[11] W.S. Chang and S.J. Na, Prediction of laser spot weld shape by numerical analysis and neural network, *Metallurgical and Material Transactions B*, 32B, pp 723-731, August 2001.

[12] J. Sabbaghzadeh, M. Azizi and M.J. Torkamany, Numerical and experimental investigation of seam welding with a pulsed laser, *Journal of Optics & Laser Technology*, 40, pp. 289-296, 2008.

[13] R. Spina, L. Tricarico, G. Basile and T. Sibillano, Thermo-mechanical modeling of laser welding of AA5083 sheets, *Journal of Materials Processing Technology*, 191, pp. 215-219, 2007.

[14] G. Tsoukantas and G. Chryssolouris, Theoretical and experimental analysis of the remote welding process on thin, lap-joined AISI 304 sheets, *International Journal of Advanced Manufacturing Technology*, 35(9 – 10), pp. 880 – 894, 2008.

[15] J. Xie and A. Kar, Laser Welding of Thin Sheet Steel with Surface Oxidation, *Welding Research Supplement*, 78, pp. 343s – 348s, 1999.

[16] S.A. Tsirkas, P. Papanikos and Th. Kermanidis, Numerical simulation of the laser welding process in butt-joint specimens, *Journal of Materials Processing Technology*, 134, pp 59-69, 2003.

Nallathambi Siva Shanmugam was born in Tiruchirappalli, INDIA on 16 November 1980. He received his Bachelor degree in Mechanical Engineering from Bharathidasan University, INDIA in 2002. He was awarded Master degree in CAD/CAM from Anna University, INDIA in 2004. He received his Doctoral degree in Finite Element Simulation pertaining to Laser Beam Welding process from National Institute of Technology (NIT) Tiruchirappalli, INDIA in 2012. His field of interest includes Finite Element Simulation on Laser Beam Welding, Friction Stir Welding, TIG welding and Bio-Mechanical Engineering.

Gengusamy Buvanashekaran received his integrated M.S. (Engg.) in Welding Technology from Slovak Technical University (SVST), BRATISLAVA in 1981 with honours. In 1995 he obtained his Ph.D on Submerged Arc Welding fluxes from Bharathidasan University, INDIA. Presently, he is working as an Additional General Manager at Welding Research Institute (WRI), BHEL, INDIA. His research interest encircles - the area of High Energy Beam processes like LASER and ELECTRON BEAM.

Krishnasamy Sankaranarayanasamy is Professor of Mechanical Engineering at National Institute of Technology Tiruchirappalli, INDIA received his B.E (Hons) in 1981 from PSG College of Technology, INDIA. He received his M.Tech in 1983 and Ph.D in 1989 from Indian Institute of Technology Madras, INDIA. His area of research mainly focuses on Laser Materials Processing, Industrial safety and Optimization in Design.